Journal of Food and Nutrition Research, 2014, Vol. 2, No. 9, 567-574
Available online at http://pubs.sciepub.com/jfnr/2/9/7

DOI:10.12691/jfnr-2-9-7

Flow Field Analysis and Defrosting Cycle Optimization in a Large-scale Industrial Cold- storage Facility

Enhai Liu[1], Tingting Yu[1], Shengyong Liu[2,*], Hongwei Liu[1]

[1]School of Energy and Building Environment Engineering, Henan University of Urban Construction, Pingdingshan, China
[2]Key Laboratory of Renewable Energy of Ministry of Agriculture, Henan Agricultural University, Zhengzhou, China
*Corresponding author: ndshyliu@163.com

Received July 03, 2014; Revised September 01, 2014; Accepted September 03, 2014

Abstract We report a joint theoretical and experiment analysis of an industrial cold-storage unit for a large-scale poultry processing enterprise in the Central Plains Economic Zone of China. The flow field inside the unit was analyzed using computational fluid dynamics, which identified an optimum forced air supply of 2.05 m s^{-1}. The defrosting cycle was then optimized experimentally, resulting in an improved defrosting method and a monthly saving of 5,530 RMB in electricity costs. Furthermore, we achieved a reduction in the temperature variation of 1.82% and in the coefficient of performance variation of 1.89%. The refrigerating capacity and electricity costs per unit of production were decreased by 8.30% and 10.20%, respectively.

Keywords: *cold storage, numerical simulation, flow-field characteristics, defrosting cycle, optimization*

Cite This Article: Enhai Liu, Tingting Yu, Shengyong Liu, and Hongwei Liu, "Flow Field Analysis and Defrosting Cycle Optimization in a Large-scale Industrial Cold- storage Facility." *Journal of Food and Nutrition Research*, vol. 2, no. 9 (2014): 567-574. doi: 10.12691/jfnr-2-9-7.

1. Introduction

We report an investigation of the flow-field characteristics of a cold-storage system, together with an experimental analysis of the defrosting cycle, for a large-scale poultry processing plant in the Central Plains Economic Zone of China. This plant processes 22.5 tons per day and has five production lines. Energy consumption is a significant issue, and improving the energy efficiency is of considerable importance. Cold-storage systems with an optimized flow field may enable more efficient distribution of heat exchange rates. Currently, air-cooling is commonly used in heat-exchange equipment in the food industry; however, problems with frost can significantly affect the food quality as well as the energy consumption.

In recent years, there have been many studies of the flow-field distribution characteristics of cold-storage units using computational fluid dynamics (CFD). The factors influencing the heat-transfer coefficient frosting behavior of cold-storage systems have been analyzed based on heat-transfer theory (Wang et al., 1998; Hu et al., 2001; Rouaud et al., 2002; Smale et al., 2006; Zhou et al., 2006; Yang et al., 2007; Demir et al., 2010; Ho et al., 2010; Solmus et al., 2012). Chourasis and Goswami (2007) investigated the flow fields of cold-storage units, including the resulting heat transfer and moisture loss, using the two-dimensional steady-state distribution parameter method; the average velocity, temperature, and ±0.61%, respectively. Chourasis et al. (2007) investigated heat and mass transfer problems related to the food-delivery process. Nahor et al. (2005) developed a transient three-dimensional CFD model to calculate the velocity, temperature, and moisture distribution in both empty and loaded cold-storage systems, with an average accuracy of ±22% for the air velocity for empty cold storage and ±20% for loaded cold storage. Foster et al. (2002, 2003) reported a number of studies concerning air infiltration in cold storage using CFD simulations. Xie et al. (2005) reported a numerical method for two- and three-dimensional studies of the airflow distribution in a fruit and vegetable cold-storage facility, and proposed modifications to cold-storage designs to improve the flow distribution. They also experimentally investigated the defrosting processes at various temperatures, and analyzed the distribution of the electrical heating parts. Wang et al. (1995) found a sub-zero flow field within a two-dimensional simulation, showing that there was a reflux flow field in the centre and that the mainstream flow was close to the edge of the unit; this behavior was exhibited by both the horizontal and vertical velocities, and was significant at both sides of the unit and to a lesser extent in the middle. Frosting was a common phenomenon during a freezing period, and must be periodically removed. There were many studies showed that the improved defrosting method would be helpful to cut down defrosting time, increase the efficiency of refrigeration equipment (Krakow et al., 1992; Hoffenbecker et al., 2005; Huang et al., 2009; Lenic et al., 2009; Bansal et al., 2010). Mao et al. (1999) analyzed frosting characteristics and heat transfer on a flat under freezer operating conditions. Sung et al. (2002) analyzed hydrophilic surfaces, which influence the frosting behavior, and investigated the effects of a hydrophobic surface on frosting. The issues faced in the

conventional (EHD) method were described, and various defrosting methods were compared. Deng et al. (2003) studied the performance of air cooler under frosting conditions by the experimentation. Liu et al. (2005) also presented transient distributed model of frost on heat pump evaporators. Wan et al. (2008) proposed a simple model to calculate the defrosting electrical energy input. Zhang et al. (2009) studied the frost accumulation on tube-fin evaporators designed for household appliances and analyzed air-side performance evaluation of three types of heat exchangers. Yin et al. (2012) proposed a novel defrosting method with an air bypass circulation system and an electric heater and described its effects on frosting.

However, research into the flow-field distribution characteristics of cold-storage units has yet to yield an adequate description of the optimum defrosting methods, allowing for economical operation of units of the scale of the Central Plains Economic Zone large-scale poultry processing plant. Here, we focus on the defrosting and flow-field characteristics of this large-scale plant, considering the effects of the slaughtering and processing of poultry.

2. Physical and Mathematical Model

2.1. Simplified Model

We used the k-ε turbulence model to simulate the flow-field characteristics of the cold-storage unit with the computational fluid dynamics (CFD) package FLUENT. Preliminary simulations were carried out to determine the most significant factors affecting the operation of the refrigeration facility. To obtain the temperature and velocity fields, we first established the appropriate mathematical model to describe the flow field and heat transfer in the cold-storage unit based on the following assumptions

(1) The products in the cold storage do not affect the flow field.

(2) The air inside the cold storage is considered to be an incompressible ideal fluid.

(3) The model of the cold-storage unit can be simplified to a three-dimensional problem without considering the impact of the goods.

(4) The cold storage, for the closed space, no considering heat and mass transfer between maintenance structure and the ambient environment.

2.2. Model Description

2.2.1. Mathematical Model

The continuity, momentum, turbulent kinetic energy (k), and turbulent dissipation (ε) equations were solved using FLUENT.

$$div(\rho\bar{u}\phi) = div(\Gamma_\phi grad\phi) + S_\phi \quad (1)$$

In formula, ϕ is the general variable, Γ_ϕ is the generalized diffusion coefficient, S_ϕ is the generalized source term. The corresponding relationship between parameters and different partial differential equations can be expressed as

Continuity equation

$$\phi = 1, \Gamma_\varphi = 0, S_\varphi = 0 \quad (2)$$

Momentum equation in x - direction: $\varphi = \mu$, $\Gamma_\varphi = \mu_{eff}$,

$$S_\varphi = -\frac{\partial p}{\partial x} + \frac{\partial}{\partial x}\left(\mu_{eff}\frac{\partial u}{\partial x}\right) + \frac{\partial}{\partial y}\left(\mu_{eff}\frac{\partial v}{\partial x}\right) + \frac{\partial}{\partial z}\left(\mu_{eff}\frac{\partial w}{\partial x}\right) \quad (3)$$

Momentum equation in y -direction: $\varphi = v$, $\Gamma_\varphi = \mu_{eff}$,

$$S_\varphi = -\frac{\partial p}{\partial x} + \frac{\partial}{\partial x}\left(\mu_{eff}\frac{\partial u}{\partial y}\right) + \frac{\partial}{\partial y}\left(\mu_{eff}\frac{\partial v}{\partial y}\right) + \frac{\partial}{\partial z}\left(\mu_{eff}\frac{\partial w}{\partial y}\right) \quad (4)$$

Momentum equation in z -direction: $\varphi = w, \Gamma_\varphi = \mu_{eff}$,

$$S_\varphi = -\frac{\partial p}{\partial x} + \frac{\partial}{\partial x}\left(\mu_{eff}\frac{\partial u}{\partial z}\right) + \frac{\partial}{\partial y}\left(\mu_{eff}\frac{\partial v}{\partial z}\right) + \frac{\partial}{\partial z}\left(\mu_{eff}\frac{\partial w}{\partial z}\right) \quad (5)$$

Energy equation:

$$\varphi = T, \Gamma_\varphi = \frac{\mu}{p_r} + \frac{\mu_t}{\delta_t}, S_\varphi = 0 \quad (6)$$

k -equation:

$$\varphi = k, \mu = \frac{\mu_t}{\delta_k}, S_\varphi = G_k - \rho\varepsilon \quad (7)$$

Where calculation on G_k, μ_t for the k -equation and ε -equation can be written as:

$$G_k = \mu_t \left\{ 2\left[\left(\frac{\partial u}{\partial x}\right)^2 + \left(\frac{\partial v}{\partial y}\right)^2 + \left(\frac{\partial w}{\partial z}\right)^2\right] + \left[\frac{\partial u}{\partial y} + \frac{\partial v}{\partial x}\right]^2 + \left(\frac{\partial u}{\partial y} + \frac{\partial w}{\partial x}\right)^2 + \left(\frac{\partial v}{\partial z} + \frac{\partial w}{\partial y}\right)^2 \right\}, \quad (8)$$

$$\mu_{ef\,f} = \mu + \mu_t, \mu_t = \rho C_\mu k^2 / \varepsilon$$

ε -equation:

$$\varphi = \varepsilon, \mu = \frac{\mu_t}{\delta_\varepsilon}, S_\varphi = \frac{\varepsilon}{k}\left(C_{1\varepsilon} - C_{2\varepsilon}\rho\varepsilon\right) \quad (9)$$

The coefficients for the $k-\varepsilon$ model are given in Table 1.

Table 1. The coefficients for the $k-\varepsilon$ model

C_μ	$C_{1\varepsilon}$	$C_{2\varepsilon}$	δ_k	δ_ε	δ_t
0.09	1.44	1.92	1.0	1.3	0.9-1.0

2.2.2. Boundary and Initial Conditions

The boundary conditions were as follows.

1. At the air-cooler outlet, the fan was set to provide forced air supply speeds of 1.5, 2.0, 2.5, and 3.0 m s^{-1}. The temperature was fixed at T=255K (−18°C). The turbulent kinetic, k, was assumed to be in the rang 0.5%-1.5% of the mean kinetic energy of the incoming flow, and the turbulent dissipation ε was given by $\varepsilon = \frac{C_\mu^{\frac{3}{4}} k^{\frac{3}{2}}}{l}$, where $l = 0.07L$ and L is the hydraulic diameter.

2. At the air-cooler return, we assumed free outflow, i.e., the velocity and pressure were unknown prior to solving the problem.

3. At the walls of the cold-storage unit, the temperature was fixed at 258K (-15°C), and no-slip boundary conditions were assumed with a wall velocity of 0 m s^{-1}.

2.2.3. Physical Model

We used a two-stage compression model based on an intermediate cooling and defrosting method with ammonia as the refrigerant. The exterior dimensions of the cold-storage unit were 13m×5m×4m. The air-cooler (Model GDJ-350, Zhejiang Xinlong Air Conditioning Equipment Co., Ltd) had exterior dimensions of 3.05 m ×0.755 m ×0.85 m, with an evaporation area of 350 m^2. Stainless steel was used to form the shelving; these storage racks were 0.6-m wide, 1.8-m high, and 2.1-m long. The physical model of the air-cooler can be simplified to a cuboid, the length, width and height are 3, 1 and 1 m, respectively.

3. Results and Analysis

3.1. CFD Simulation

Figure 1 shows the flow-field distribution of the empty cold-storage unit, and Figure 2 shows the flow field in the cold-storage facility with products on the shelving. From the velocity distributions in the empty cold-storage unit, there was a large central recirculation zone in which the velocity was small. At the corners, small ripple vortices formed, which occurred due to the cold flow around the wall surface caused by the obstacles. Figure 2 shows a width cross-section located 1.24 m from the walls where the temperature field was almost uniform; however, close to the walls, the temperature was higher, resulting in a significant temperature gradient in this area. As the outlet fan speed increased, the recirculation region gradually expanded, and the flow approached closer to the walls, giving a more uniform temperature distribution. These simulated data show that the outlet fan speed significantly affected both the velocity and temperature fields inside the cooler. Furthermore, there were numerous low-energy eddies, which formed due to the flow around the walls of the cold-storage unit and the shelving. Larger velocities increased the mainstream flow field and reduced the eddy currents.

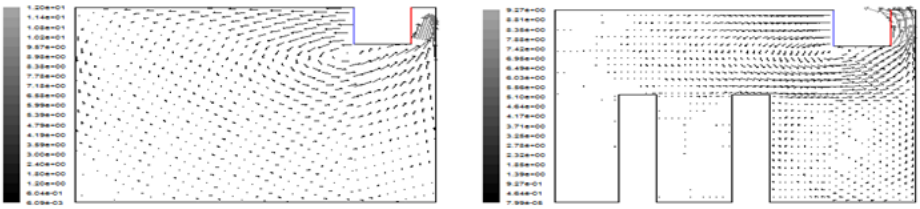

（a）the velocity field in the cold storage (the velocity of the cold fan is 1.5m s^{-1})

（b）the velocity field in the cold storage with the foodstuffs shelves (the velocity of the cold fan is 1.5 m s^{-1})

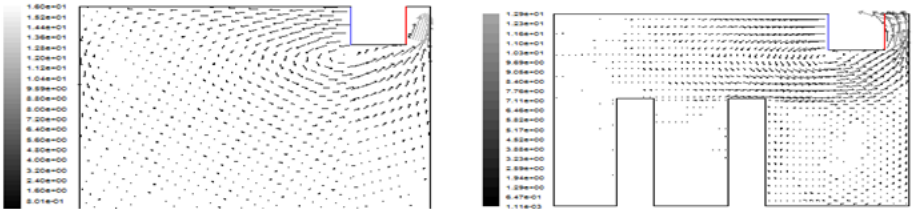

（c）the velocity field in the cold storage (the velocity of the cold fan is 2 m s^{-1})

（d）the velocity field in the cold storage with the foodstuffs shelves (the velocity of the cold fan is 2 m s^{-1})

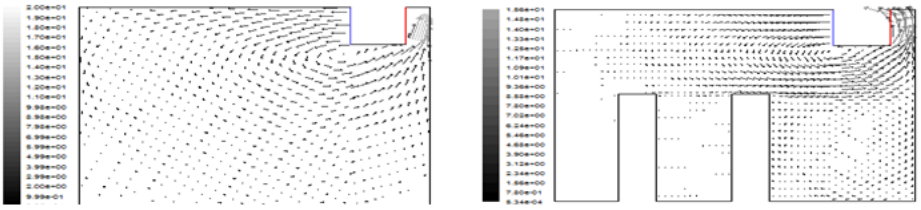

（e）the velocity field in the cold storage (the velocity of the cold fan is 2.5 m s^{-1})

（f）the velocity field in the cold storage with the foodstuffs shelves (the velocity of the cold fan is 2.5 m s^{-1})

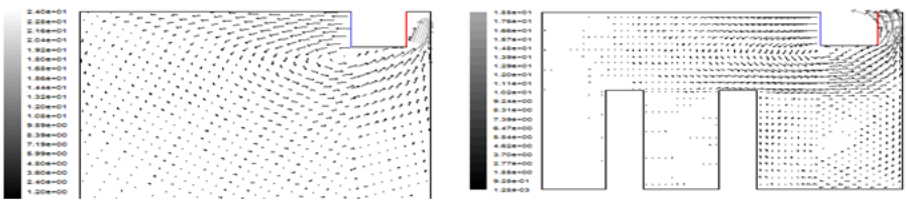

（g）the velocity field in the cold storage (the velocity of the cold fan is 3 m s^{-1})

（h） the velocity field in the cold storage with the foodstuffs shelves (the velocity of the cold fan is 3 m s^{-1})

Figure 1. The velocity fields of the cold storage at Y=1m (the cross section of 1m from the ground)

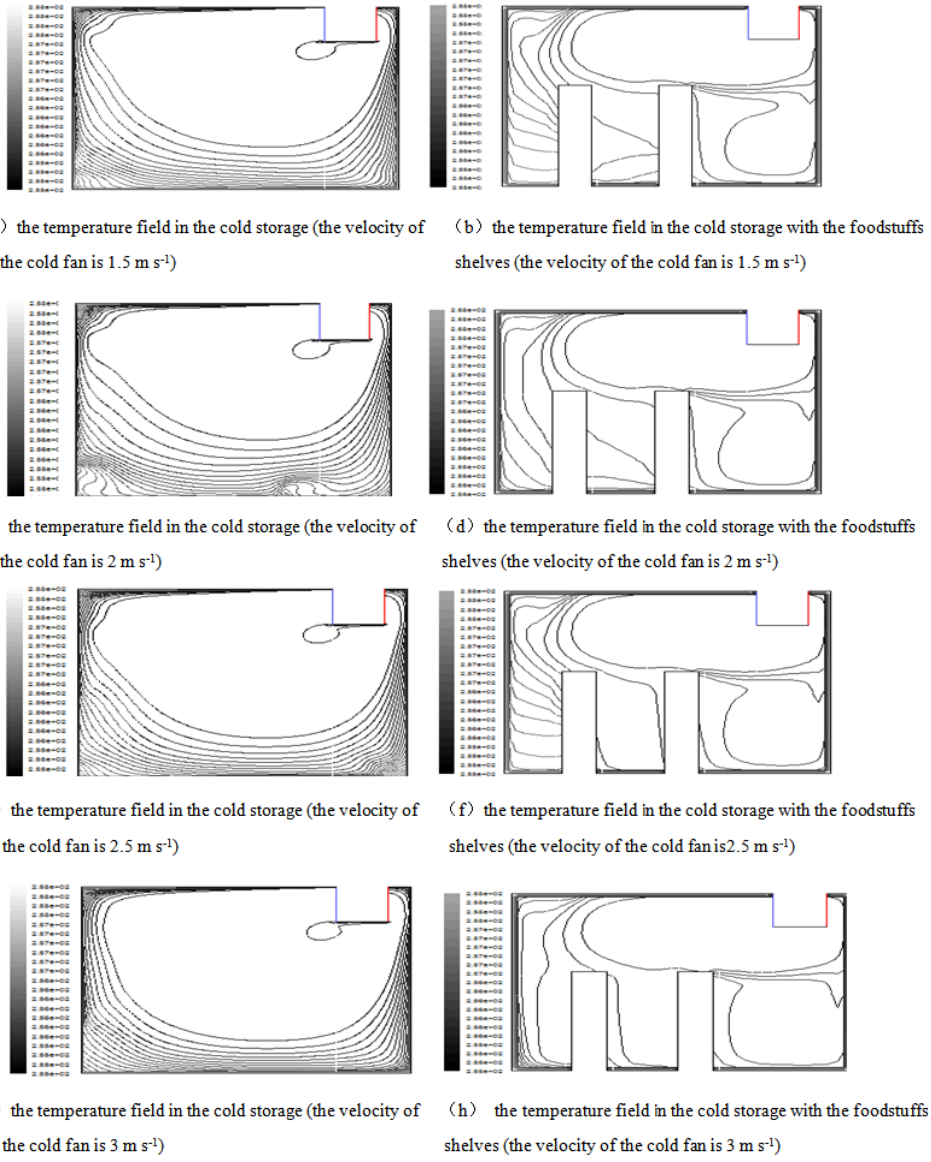

（a）the temperature field in the cold storage (the velocity of the cold fan is 1.5 m s^{-1})

（b）the temperature field in the cold storage with the foodstuffs shelves (the velocity of the cold fan is 1.5 m s^{-1})

（c）the temperature field in the cold storage (the velocity of the cold fan is 2 m s^{-1})

（d）the temperature field in the cold storage with the foodstuffs shelves (the velocity of the cold fan is 2 m s^{-1})

（e）the temperature field in the cold storage (the velocity of the cold fan is 2.5 m s^{-1})

（f）the temperature field in the cold storage with the foodstuffs shelves (the velocity of the cold fan is2.5 m s^{-1})

（g）the temperature field in the cold storage (the velocity of the cold fan is 3 m s^{-1})

（h） the temperature field in the cold storage with the foodstuffs shelves (the velocity of the cold fan is 3 m s^{-1})

Figure 2. The temperature fields of the cold storage at Z=1.24m: makes section 1.24m away from the width direction (z direction, x-y plane) to observe the temperature field

3.2. Analysis and Discussion

To maintain good performance in refrigeration systems, it is necessary to analyze the uniformity of the cold flow inside the cold storage. As the fan speed increased, the velocity and temperature fields varied significantly. Higher fan speeds produced more uniform velocity and temperature distributions inside the cooler, which are advantageous for cooling. However, the increased fan speed may lead to weight loss of the products due to evaporation, as well as to increased energy consumption. Further simulated and experimental data related to the costs (both in terms of energy consumption and product quality) of using a high fan speed should be performed to determine the optimum operating conditions. There is also scope to optimize the geometry of the storage on the shelving, as well as the distribution of the regions within the cold-storage facility.

The optimum fan speed was obtained based on Figs. 1d and 2d, which indicated more uniform velocity and temperature distributions. This allowed us to define the optimum design and operating conditions for the cold-storage facility.

3.3. Optimum Velocity Measurements

The freezing rate and quality of the products in the cold-storage facility are dependent on the velocity and temperature fields. A large air velocity may lead to weight loss of the products and increased energy consumption. To improve the organization of the cold-storage unit and to decrease the weight loss of the products during storage, a forced air supply of 2.05 m s^{-1} was used. This speed was based on experiments using the marine cold storage unit of the Shanghai Marine Equipment Co., Ltd, at the Henan University of Urban Construction in China. The experimental setup used in this study was a closed refrigeration system with a forced air supply, with an optimal height of 1m. The velocity was measured using a Cups Light Wind Anemometer, model DEM6: the results showed that the velocity was in agreement with the simulated data to within $\pm$0.2 m s^{-1}. The forced air supply was varied in the range 1.8 - 2.3 m s^{-1} to determine the optimum efficiency. The results satisfied the requirements of the heating, ventilation, and air-conditioning (HVAC) systems.

4. Improvement of the Defrosting Method

4.1. Proposed Experiments

Experiments were carried out to optimize the current defrosting method, which was based on hot ammonia-water defrosting. To ensure that the air-cooler was operating economically under frosting conditions, the defrosting method was analyzed experimentally. Improvements to the method were proposed, which could make the refrigeration system more effective with less product weight loss and reduced energy consumption. To maintain good performance of the heat exchanger, defrosting must be carried out periodically. Preliminary experiments showed that frost accumulated mainly on the first few central rows of the return vent of the air-cooler where the finned surface protruded further than in the previous row. Here, we analyzed the influence of the defrosting cycle period and studied methods to improve the defrosting method by considering the coupled effects of slaughtering and processing of the product during refrigeration.

Figure 3a shows photographs of frost growth at the return vent and the first few central rows of the finned surface of the air-cooler. Figure 3b shows that defrosting was not sufficient to remove the accumulated frost from all of the surfaces of the air-cooler.

（a） the frost layer at the upper part of the return vent

（b） the effects of defrosting are not sufficient to remove the frost from the entire surface of the coil air-cooler

Figure 3. Photographs of frosting

4.2. Experimental Apparatus and Test Method

The aim was to improve the overall efficiency of the refrigeration system, reducing the weight loss of the product and the total energy consumption. The defrosting device had a movable vibrating mechanism installed at the return vent of the air-cooler. Following design and manufacture, the defrosting device was operated in the cold-storage facility, which was composed of twenty-six 2.5-cm-long springs with a natural length of 15 cm, and two steel plates of dimensions 3.1 m × 0.025 m × 0.005 m with a tensile strength of 350MPa. The springs were aligned vertically between the two steel plates and were fixed to the steel plate at both ends. Figure 4 shows a schematic diagram of the experimental setup.

Prior to taking measurements, we used a 40-m-long electrically heated wire with a power density of 17 Wm^{-1} to defrost the air-cooler; this wire was embedded in the external surface of the springs and the rows of air-cooling fin-tubes. The electrically heated wire was switched on for 5 minutes during the defrosting cycle. The adjusting screws were used to close the apertures in the steel plates following defrosting for 30 min. Due to the increase in the temperature of the surface of the fins and tubes, the elastic force of the springs increased gradually over time, causing the ice layer to shatter due to the axial stress caused by its gravity and vibration.

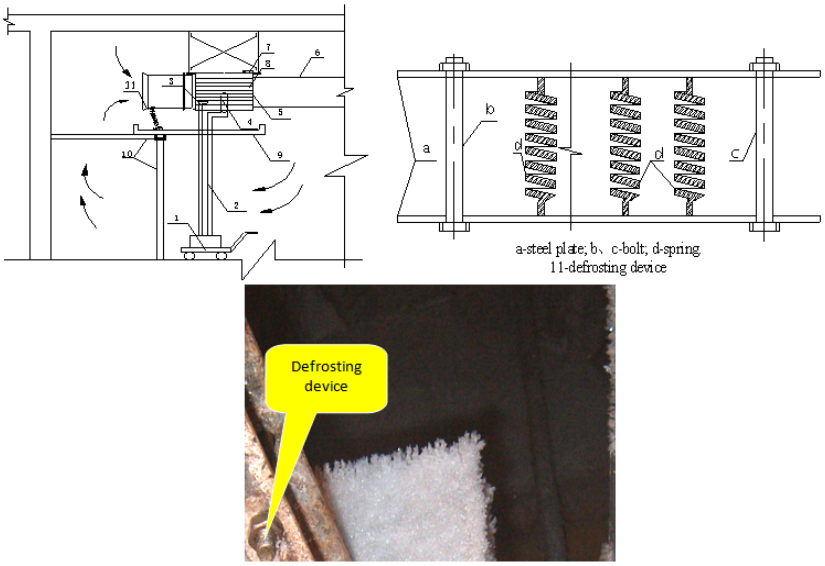

Figure 4. Schematic of experimental setup. 1- movable vibrator; 2-hose connection; 3,4- electric heating wire for defrosting; 5- cold fan; 6- blast pipe; 7- temperature sensing packet; 8-fin-tube; 9- catchment tray;10- bracket; 11- defrosting device

5. Economic Analysis

5.1. Operating Parameters

To reduce energy consumption, the refrigeration system in the experimental cold-storage unit was fitted with a screw compressor, with one middle economizer, an air cooler, an ammonia pump, an evaporative condenser, a water-circulation pump, and a water-defrosting pump. The refrigeration parameters and details of the equipment used in the experimental cold-storage unit are listed in Table 2.

5.2. Results and Discussion

Here, we provide a detailed analysis of the influence of defrosting on the performance of the cold-storage unit. We optimised the defrosting method at low temperatures, and the results were validated by comparison with experimental data. Ideally, the refrigerating system should run uninterrupted to provide optimum efficiency. The analysis showed that the improved defrosting method gave rise to less variation in the temperature (1.82%), as well to a more consistent coefficient of performance, which varied by only 1.89%, as shown in Figure 5.

Table 2. The refrigeration parameters and equipments of the experimental cold storage

Devices	The number of operational equipments	The matching motor power
The low stage compressor	3	3×100 kW(300 kW)
The high stage compressor	1	1×250 kW(250 kW)
The air cooler	3	3×2×1.1kW(6.6 kW)
The water circulating pump	2	2×11 kW(22 kW)
The water defrosting pump	3	1×11 kW, 2×3 kW(17 kW)
The ammonia pump	2	2×5.5 kW(11 kW)
The evaporative condenser	2	2×18 kW(36 kW)

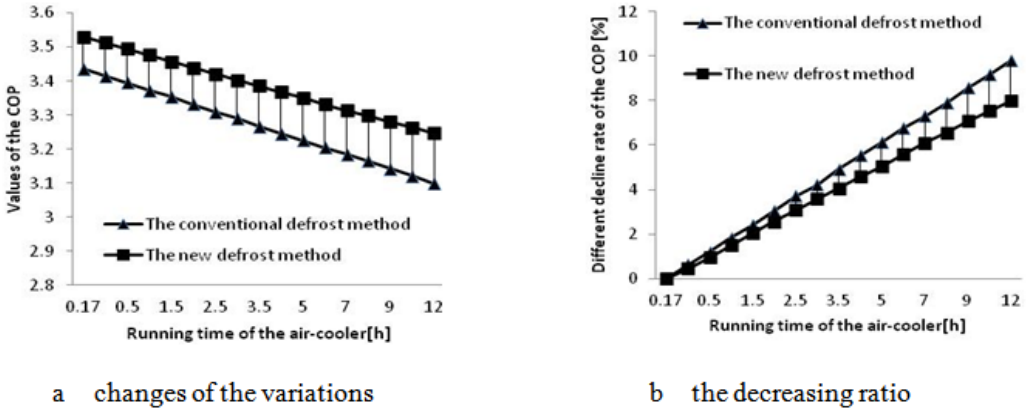

a changes of the variations b the decreasing ratio

Figure 5. Changes of the variations and the decreasing ratio on coefficient of performance

We found that the quality of the frozen food was sensitive to both the storage temperature and to fluctuations in this temperature. Therefore, the temperature and relative humidity of the cold-storage unit must be maintained at prescribed levels during the defrosting cycle of the air-cooler. Based on the operational records of the cold-storage unit, the improved defrosting method was shown to be both feasible and effective. These results were validated by comparison with experimental data.

It is desirable to achieve continuous freezing, reduce the duration of the defrosting cycle, and increase the overall efficiency of refrigeration equipment. The capacity of the cold storage facility in the Central Plains Economic Zone is 22.5 tons per day, and the power consumption is 100 kW. The modified defrosting method resulted in a freezing time of 11 hours and a defrosting time of 1.33 hours, which represents reductions of 1 hour and 1.17 hours, respectively.

According to the above analysis, the heat-transfer coefficient of the air cooler and the refrigeration capacity were increased through the use of the new defrosting method.

The energy consumption of the refrigerating unit is given by

$$Q = \frac{Q_m}{G} \tag{10}$$

and the capacity of the refrigerating unit is given by

$$Q_m = Q_d \times n \times t \times 3600 \tag{11}$$

where Q is the capacity of the screw compressor, Q_m is the product capacity per month, Q_d is the product capacity per day, t is the time for freezing, n is the product freezing frequency per month, and G is the product freezing capacity per month.

The power consumption per unit of product is given by

$$C_e = C_{e1} + C_{e2} - C_{e3} \tag{12}$$

$$C_m = nRC_e \tag{13}$$

where C_e is the overall reduction in electrical power, C_{e1}, C_{e2}, and C_{e3} are the electricity consumption during freezing, and the power consumption of the electrically heated wire and the defrosting pump, C_m is the savings in terms of cost of electricity, and R is the local electrovalence.

Based on the experimental data and the records of the cold-storage unit, and following from equations (10) through (13), the calculated energy consumption was 178,200,00 kJ, and the freezing capacity per month was 675 tons. The energy consumption per ton of product was therefore 264,000 kJ per ton. Compared with the conventional defrosting method (i.e., hot ammonia

defrosting), the defrosting time of the new method was reduced by 1.17 hours, and the defrosting efficiency increased by 53.2%, which resulted in less variation in the temperature and the coefficient of performance (which varied by 1.82% and 1.89%, respectively). The refrigerating capacity and electricity cost per unit of production decreased by 8.30% and 10.20%, respectively. These results show that the modified defrosting method resulted in a monthly saving of 5,530 RMB in electricity charges.

6. Conclusions

A joint theoretical and experimental investigation of the energy consumption and thermal performance of an industrial cold-storage unit was carried out. The velocity and temperature distributions were calculated using CFD at a range of airflow conditions. The simulated data indicated that the structure could be improved, and the distribution of products in the cold-storage unit was optimised. An experimental analysis resulted in an optimised defrosting method, which was designed considering the slaughtering and processing activities in the refrigerated environment.

The major conclusions of this work can be summarized as follows.

(1) A numerical simulation of the flow field of the empty cold storage with a forced air supply was carried out at velocities of 1.5, 2.0, 2.5, and 3.0 m s^{-1}. The velocity varied more strongly near the walls of the cold-storage unit, as well as near the air-cooler. There was a large circumfluence in the flow field of the cold-storage unit, which was detrimental for the cold storage of foodstuffs. The mainstream of the flow field was close to the walls of the cold-storage unit; at a width cross-section located 1.24 m from the walls, the flow field distribution was the most continuous and uniform.

(2) Based on the simulated data, the velocity and temperature fields varied strongly as a function of the velocity of the cold-air fan, and there were many low-energy eddies at low fan speeds. Greater fan velocities led to more coverage of the shelving (i.e., food storage region) by the mainstream of the flow field and smaller eddies. To reduce the product weight loss and save energy, an optimum fan speed of 2.05 m s^{-1} was identified.

(3) A new defrosting method was described, and the experimental results demonstrated that it resulted in a savings of 5,530 RMB in electricity costs per month. Furthermore, the modified defrosting method also reduced the temperature variation by 1.82% and coefficient of performance variation by 1.89%. An increase in the defrosting efficiency of up to 53.2% was observed. The refrigerating capacity and electricity charge per unit of production decreased by 8.30% and 10.20%, respectively, following implementation of the optimisation strategies described here.

Acknowledgment

This work was supported by the Henan Province Basic and Frontier Technology Research Program (122300410086) and Henan Key Scientific and Technological Program (132102210148) of China.

References

[1] Bansal, P., Fothergill, D., Fernandes, R., 2010. Thermal analysis of the defrost cycle in a domestic freezer. International Journal of Refrigeration 33 (3), 589-599.

[2] Chourasia, M.K., Goswami, T.K., 2007. Steady state CFD modeling of airflow, heat transfer and moisture loss in a commercial potato cold store. International Journal of Refrigeration. 30, 672-689.

[3] Chourasia, M.K., Goswami, T.K., 2007. Three dimensional modeling on airflow, heat and mass transfer in partially impermeable enclosure containing agricultural produce during natural convective cooling. Energy Conversion and Management. 48, 2136-2149.

[4] Demir, H., Mobedi, M., Ulku, S., 2010. The use of metal piece additives to enhance heat transfer rate through an unconsolidated adsorbent bed. Int. J. Refrigeration 33, 714-720.

[5] Deng, D., Xu, L., Xu, S., 2003. Experimental investigation on the performance of air cooler under frosting conditions. Appl. Therm. Eng. 23, 905-912.

[6] Foster, A.M., Barrett, S.J., James, J., Swain, M.J., 2002. Measurement and prediction of air movement through doorways in refrigerated rooms. International Journal of Refrigeration 25 (8), 1102-1109.

[7] Foster, A.M., Swain, M.J., Barrett, R., James, S.J., 2003. Experimental verification of analytical and CFD predictions of infiltration through cold store entrances. International Journal of Refrigeration 26 (8), 918-925.

[8] Ho, S.H., Rosario, L., Rahman, M.M., 2010. Numerical simulation of temperature and velocity in a refrigerated warehouse. International Journal of Refrigeration 33, 1015-1025.

[9] Hoffenbecker, N., Klein, S.A., Reindl, D.T., 2005. Hot gas defrost model development and validation. Int. J. Refrigeration 28,605–15.

[10] Hu, Z., Sun, D.W., 2001. Predicting local surface heat transfer coefficients by different turbulent $k-\varepsilon$ models to simulate heat and moisture transfer during air-blast chilling. Int. J. Refrigeration 24, 702-717.

[11] Huang, D., Li, Q., Yuan, X., 2009. Comparison between hot-gas bypass defrosting and reverse-cycle defrosting methods on an air-to-water heat pump. Applied Energy 86 (9), 1697-1703.

[12] Krakow, K.I., Yan, L., Lin, S.A., 1992. Model of hot-gas defrosting of evaporators-Part 1: heat and mass transfer theory ASHRAE Trans 98 Part 1 451-461.

[13] Lenic, K., Trp, A., Frankovic, B., 2009. Prediction of an effective cooling output of the fin-and-tube heat exchanger under frosting conditions. Appl. Therm. Eng. 29, 2534-2543.

[14] Liu, Z., Zhu, H., Wang, H., 2005. Study on transient distributed model of frost on heat pump evaporators. J. Asian. Archit. Build Eng. 4, 265-270.

[15] Mao, Y., Besant, R.W., Chen, H., 1999. Frosting characteristics and heat transfer on a flat under freezer operating conditions: Part 1, Experimentation and correlations. ASHRAE Trans. 105, 231-251.

[16] Nahor, H.B., Hoang, M.L., Verboven, P., Baelmans, M., Nicolaï, B.M., 2005. CFD model of the airflow, heat and mass transfer in cool stores. International Journal of Refrigeration 28, 368-380.

[17] Rouaud, O., Haver,M., 2002. Computation of the air flow in a pilot scale clean room using $k-\varepsilon$ turbulence models. Int. J. Refrigeration 25, 351-361.

[18] Smale, N.J., Moureh, J., Cortella, G., 2006. A review of numerical models of airflow in refrigerated food applications. International Journal of Refrigeration 29 (6), 911-930.

[19] Solmus, I., Rees, D.A.S., Yamalı, C., Baker, D., Kaftanoglu, B., 2012. Numerical investigation of coupled heat and mass transfer inside the adsorbent bed of an adsorption cooling unit. Int. J. Refrigeration 35, 652-662.

[20] Sung, Jhee., Kwan-Soo, Lee., Woo-Seung, Kim., 2002. Effect of surface treatments on the frosting/defrosting behavior of a fin-tube heat exchanger. International Journal of Refrigeration 25, 1047-1053.

[21] Wan, J.K., Zhang, Q., Cao, G.R., 2008. A simple model to calculate the defrosting electrical energy input and the ways to optimize the air cooler's electro-thermal defrosting system. Journal of Shanghai Fisheries University 17 (2), 227-231.

[22] Wang, CC., Chang, CT., 1998. Heat and mass transfer for plate fin-and-tube heat exchangers, with and without hydrophilic coating. Int J Heat Mass Transfer 41, 3109-3120.

[23] Wang, J.F., Hu, X.F., Liu, C.Y., Jiang, W.Q., 1995. Air field simulation of freezing store. Cold storage Technology 4, 4-17(in Chinese).

[24] Xie, J., Qu X.H., Xu S.Q., 2005. Numerical simulation and verification of airflow in cold-store. Transactions of The Chinese Society of Agricultural Engineering 21, 11-15.

[25] Xie, J., Qu X.H., Shi J.Y., Sun, D.W., 2006. Effects of design parameters on flow and temperature fields of a cold store by CFD simulation. J Food Eng 77, 355-363.

[26] Yang, Z., Xu, XL., Li, XH., 2007. Simulation and experiment on the unsteady 3D flow field of cool store. J Tianjing Univ Sci Technol 40, 157-162.

[27] Yin, H.J., Yang, Z., Chen, A.Q., Zhang, N., 2012. Experimental research on a novel cold storage defrost method based on air bypass circulation and electric heater. Energy 37, 623-631.

[28] Zhang, P., Hrnjak, P.S., 2009. Air-side performance evaluation of three types of heat exchangers in dry, wet and periodic frosting conditions. Int. J. Refrigeration 32, 911-921.

[29] Zhou, G., Zhang, Y., 2006. Numerical and experimental investigation on the performance of coiled adiabatic capillary tubes. Appl. Thermal Eng. 26, 1106-1114.

Nomenclature

ϕ general variable δ_t constant, its value is 0.9-1.0

Γ_ϕ diffusion coefficient δ_k, δ_ε constant

S_ϕ source term P_r Prandtl number

μ molecular viscosity[kg (m s)$^{-1}$] G_k turbulent generation rate [N (m^{-2} s)]

μ_{eff} effective viscosity[kg (m s)$^{-1}$] ε turbulence energy dissipation rate (m^2 s^{-3})

μ_t turbulent viscosity[kg (m s)$^{-1}$] ν kinematic viscosity(m^2 s^{-1})

u, υ, w different velocity in x, y, z-direction(m s^{-1})

x, y, z x, y, z coordinate(m) T temperature(°C)

C_μ turbulence model coefficient $C_{1\varepsilon}$, $C_{2\varepsilon}$ constant

ρ fluid density(kg m^{-3}) k kinetic energy of turbulence (m^2 s^{-2})

Q refrigerating capacity(kW) t time of a freezing period(h)

Q_m refrigerating capacity of the products per month(kW/m)

Q_d refrigerating capacity of the products each day(kW/d)

G freezing capacity of the products each month(ton)

C_e value of the operation electricity can be saved(kW h)

C_{e1} value of the refrigerating electricity during a freezing period(kW h)

C_{e2} power consumption of the electric heating wire(kW h)

C_{e3} power consumption of the water defrosting pump(kW h)

C_m electricity charge can be saved(RMB)

R local electrovalence(RMB)